UNIVERSITY OF LIVERPOOL

ATLAS
INDET–NO–192

25 November 1997

Study of the annealing effects on irradiated n^+n silicon detectors for ATLAS

P.P. Allport, P.S.L. Booth, C. Green, A.Greenall, J.N. Jackson,
T.J. Jones, J.D. Richardson, S. Martí i García[1], N.A. Smith

Physics Department, Oliver Lodge laboratory, University of Liverpool,
Oxford Street, Liverpool L69 7ZE, U.K.

Abstract

The performance of the n^+n silicon micro-strip detectors for the ATLAS forward region has been studied after being subject to irradiation with 2×10^{14} protons/cm^2 and a period of annealing lasting 35 days at 20°C. As consequence of the irradiation damage, the signal to noise ratio is degraded due to charge trapping. The net effects of the subsequent annealing were both a reduction of the reverse current and a change of the full charge collection voltage, decreasing first thanks to the beneficial annealing and increasing afterwards enhanced by the long term annealing. No effect on the charge collection efficiency was appreciated due to the annealing. The response of the irradiated n^+n detectors still ensuring a successful operation, even after 10 years of LHC running.

[1] e-mail address for correspondence: martis@hep.ph.liv.ac.uk

1 Introduction

ATLAS [1] is a general purpose experiment for the LHC. The LHC is a proton-proton collider which will operate in the 27 km circumference of the LEP tunnel at CERN. The extremely high energy collisions of the LHC (7.7 TeV per beam) together with its luminosity (10^{34} cm^{-2}s^{-1}) will open a new domain of experimental high energy physics exploration. In order to achieve its physics objectives, ATLAS must incorporate an inner tracking detector which should be capable of accurate track reconstruction for high precision momentum measurement. Also required is a rigorous determination of the impact parameter of the particles generated in the collision, and in the subsequent decays of long lived particles generating secondary vertices. These properties should be guaranteed even for detectors operating immersed in a high radiation environment, and for at least ten years of LHC operation. This represents a serious constraint for the ATLAS inner tracker, as the high dose at which the detectors will be exposed (equivalent to 1.5×10^{14} 1-MeV-neutron/cm^2) will deteriorate their performance. There are no realistic prospects for replacing the ATLAS tracking system during the lifetime of the experiment. For this reason ATLAS will be equipped with detectors designed to withstand the radiation damage and tested in advance to certify their radiation hardness.

The effects of the radiation on silicon detectors can affect both: bulk and surface. The defects of the bulk [2, 3, 4, 5] are mainly caused by charged and neutral hadrons and due to the non ionizing energy loss (NIEL) of those particles. NIEL is used in the displacement of atoms in the lattice. The bulk damage has a considerable influence on the leakage current, the effective doping concentration and may lead to charge trapping. A large increase in the current results in greater noise, heat and power consumption. The change on the effective doping concentration affects the operation voltage. Charge trapping degrades the collection of the charge produced by ionization, thus affecting the size of the signal. In addition defects at the bulk-insulator interface significantly alter the device surface properties.

Although the silicon detectors of the ATLAS inner tracker will operate at low temperature, there are foreseen several warm up periods during the technical stops, thus triggering the annealing and recombination of the defects originated by the radiation. For that reason it is important to understand how the annealing influences the operational properties of the irradiated detectors. Annealing will alter primarily the leakage current, the depletion and the full charge collection voltage. The radiation effects can be split into three components [5, 6]: short term, long term and permanent. The short term damage can be overdue after a short annealing period. The long term annealing effect has a harmful influence over the detector's properties, affecting mainly the depletion voltage.

The noise and the signal to noise ratio of the silicon detectors depend on the read out sampling time. In LHC the beams will collide every 25 ns. Consequently, the use of the appropriate read out electronics is essential for this study. Analogue read out allows measuring the exact amount of collected charge and the noise level.

The aim of this article is to study the performance of a full size n^+n silicon detector of the ATLAS forward tracking system irradiated with a dose equivalent of 10 years of LHC operation, and then subject to an annealing cycle of 35 days at 20°C.

2 Prototype and Experimental Set-up

In this section the ATLAS wedge n^+n silicon micro-strip detector and the basic features of the FELIX 128 channel analogue read out chip are described. Details are also given for the irradiation, annealing cycle and bonding scheme.

The Prototype. The detector used in the present study is a wedge shaped detector of 64 mm and 56 mm width and 64 mm length, with a read out pitch varying with the fan from 70μm to 80μm, manufactured by Hamamatsu. The strips are n^+-type in a n-type bulk[1], AC coupled (figure 1). These strips are connected together to a bias ring through a polysilicon resistor (600 KΩ). When biasing the detector the n^+ strips were directly grounded and the p-type backplane was connected to a negative bias voltage. Both sides of the detector are surrounded by five guard rings. Their function is used to shield the sensitive part of the detectors and to provide a gradual drop of the edge potential, even after irradiation. Around the n^+ strips, an individual p-stop isolation frame is used to interrupt the accumulation layer of electrons at the oxide boundary which would otherwise short the n^+ strips together. From the point of view of concerns relating to high fields (e.g. micro-discharges [7]), it is important to know the relative position of the implant and the metal contact. In this case, the size of the metal contact is smaller by 2μm.

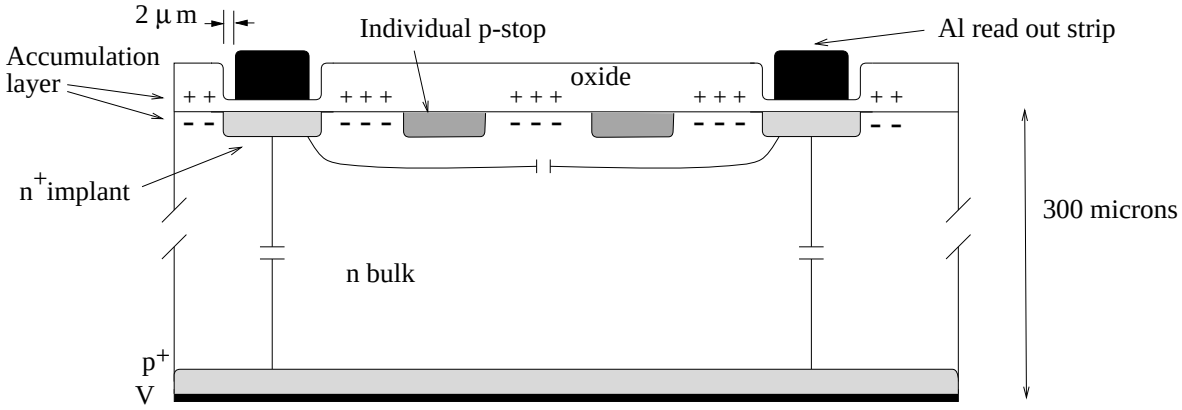

Figure 1: Schematic view of the n^+n detector cross section.

[1] The choice of read out he n-side was motivated by the possibility of operating the detector partially depleted.

FELIX Analogue Read Out Chip. The FELIX chip [8] is a 128 channel integrated circuit designed to read out silicon strip detectors of the LHC. The architecture of the device can be broken down into 3 main blocks: a) front end pre-amplifier and shaper with a CR-RC characteristic of 75 ns peaking time; b) an analogue delay buffer 1.6μs deep; c) an Analogue Pulse Signal Processor (APSP). The chip has been designed to run in two modes:

- *Deconvolution*: the collected charge in one strip is obtained from a suitable weight of three 25 ns consecutive measurements [9]. It allows the extraction of the charge deposition in a single beam crossing, even in the case of pile-up of events, as required for the high luminosity running of LHC.
- *Peak*: The charge collected is obtained for each event from the measurement of the height of the signal pulse. It requires a minimum time of 75 ns between two consecutive pulses, in order to avoid the pulse pile-up.

The Trigger System. The trigger system for the radioactive source and cosmic ray runs was based on the coincidences of two scintillators located above and below the silicon micro-strip detector. The coincidences are triggered by the $\sim$ 2 MeV electrons (minimum ionizing particles) from a ^{106}Ru source decay chain. For noise and calibration runs, the trigger signal was produced by a synchronised pulse generator.

The Irradiation. The detectors were irradiated using the 24 GeV proton beam of the PS accelerator complex at CERN. The integrated dose was 2×10^{14} protons/cm^2. The scaling factor of the damage induced by the NIEL of 24 GeV protons is 0.6 that of the 1 MeV neutrons [6].

In order to avoid the annealing effects taking place before bringing the detectors back to the home laboratory, they were kept cold at a temperature of -5°C during irradiation and afterwards stored at -10°C in the University of Liverpool laboratory. Detectors were warmed up to room temperature only for few hours during wire bonding to the read out electronics.

The Annealing Cycle. After being irradiated, one detector was subject to several cycles of annealing, each one lasting for various days. During every cycle the temperature of the detector was kept constant at 20°C inside a climate box equipped with a temperature controller. The cycles were chosen in such a way that corresponded with: 1, 3, 5, 7, 9, 13, 18, 24 and 35 days of isothermal annealing. The results obtained prior the annealing cycle started, are labelled as day 0.

At the end of each cycle and in order to suspend the annealing process, the detectors were stored again in the cold chamber at -10°C during the measurements, thus limiting the diode reverse current.

The Bonding Scheme. As the full size of the ATLAS forward tracking modules will be 12 cm (two 6cm-detectors bonded together), the correct input load was simulated with only one detector by connecting half of the 128 channels directly bonded to the FELIX to a further set of non-adjacent 64 strips. With this configuration, 192 strips were connected but read out only through 128 channels.

The 128 read out channels were grouped in 4 groups of 6cm, 12cm, 12cm and 6cm. The noise in the 12cm region is seen to be higher than that of the 6cm region as expected from the greater capacitive load (figure 2).

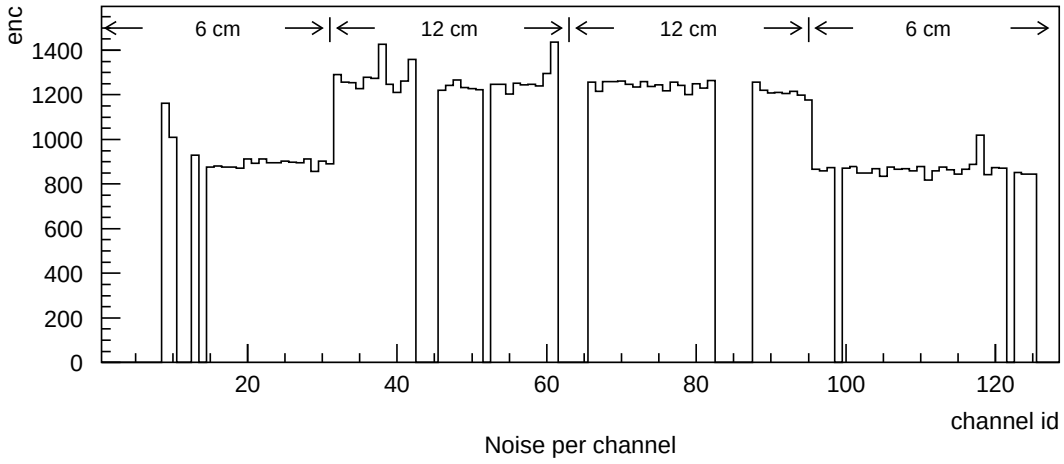

Figure 2: Noise per channel in peak mode when biasing the detector with 250 V and after 18 days of annealing at 20°C. Some channels are masked due to faulty bonds and noisy channels. The noise of those masked channels is set to zero. The range of the four groups of channels are also indicated.

When correcting for the *common mode* (coherent noise due to common pick up) each of the four 32-channel groups was treated independently from the others. Those channels with known problems were removed from the common mode calculation (see figure 2 for a list of masked channels). Some of those channels were removed because they never gave signal during a source run due to a faulty bond (11 out of 128) and some others because they were considered noisy (18 out of 128). The value of the common mode noise was seen to depend on both read out mode and strip length (see table 1).

3 Detector Performance

The performance of the irradiated detectors was studied taking into consideration the following points:

- reverse bias potential (varied from 0 V up to 600 V)

Table 1: Common mode noise in electrons as extracted for the 6cm and 12cm regions and for the different FELIX read out modes.

	Common mode noise (e)	
mode	6 cm	12 cm
peak	580 ± 13	920 ± 18
deco.	1490 ± 100	2670 ± 210

- FELIX operation mode (peak and deconvolution),
- elapsed annealing time,
- strip length (6cm and 12cm)

The relevant properties for the operation of a silicon detector under study are: the leakage current, the noise, the charge collection efficiency, the required voltage for optimum charge collection and the relative particle detection efficiency. It is also worth mentioning the calibration procedure of the set of 6cm and 12cm-long channels.

3.1 Leakage Current

The leakage current of the full detector (i.e. the current flowing through strips plus guard rings) has been studied as a function of the reverse bias voltage (figure 3) and the annealing time (figure 4).

The main effect of the radiation damage was a net increase of the current by more than two orders of magnitude with respect to that of the unirradiated detector (e.g. before irradiation the current registered at 100 V was 0.5 μA, compared with the reading for the same voltage but after irradiation: 210 μA even at -10°C).

After irradiation the leakage current steadily increases with the reverse bias voltage (figure 3). No evidence of breakdown is found for voltages up to 500 V and the currents are stable and reproducible.

In terms of the current, the effect of the annealing on an irradiated detector is just a progressive reduction of that when increasing the total integrated annealing time. This is shown in both figures 3 and 4. For example, at 200 V the current is seen to decrease by a 25% after 35 days of annealing, from 281 μA to 212 μA. According to the reverse current behaviour, there is no evidence for a reverse annealing effect on the current [10].

3.2 Calibration

In order to determine the equivalence in electrons of one ADC count, it was necessary to run the system in calibration mode. In this mode a pulse is injected in 1 out of every

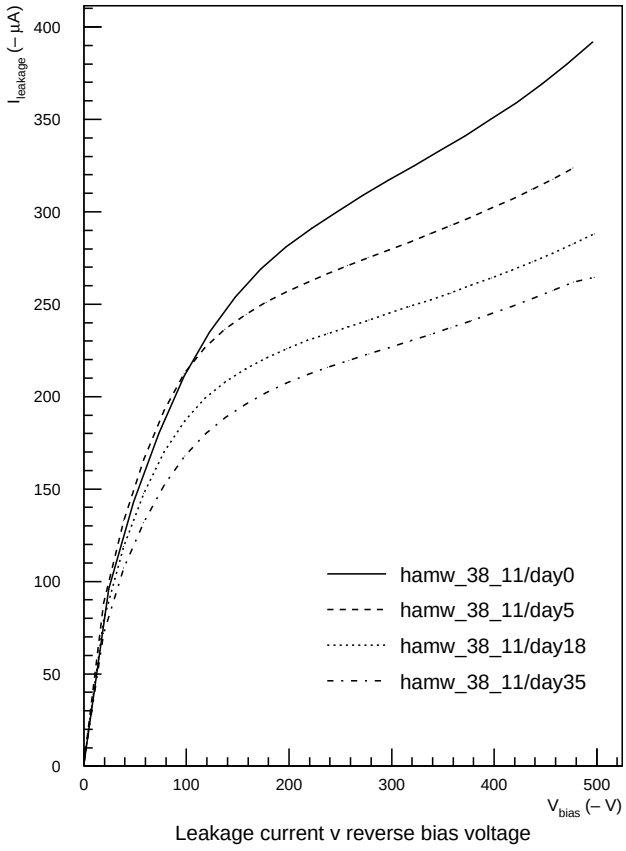

Figure 3: Leakage current of the detector (at $-10°$C) after irradiation with a dose of 2×10^{14} protons/cm^2, as a function of the reverse bias voltage and after different annealing cycles.

10 FELIX channels. The corresponding conversion figures are presented in table 2.

Table 2: Equivalence in electrons for an ADC count using the charge induced by a mip (3.6 fC) as calibrate signal.

	electrons	
mode	6cm	12 cm
peak	184.4 ± 2.9	192.3 ± 2.5
deco.	99.3 ± 2.5	115.4 ± 3.0

In its turn, the size of the calibrate input pulse was tuned in order to reproduce the peak of the Landau distribution which was obtained in a source run with an unirradiated detector of similar characteristics. The agreement in peak mode was within a 1% and

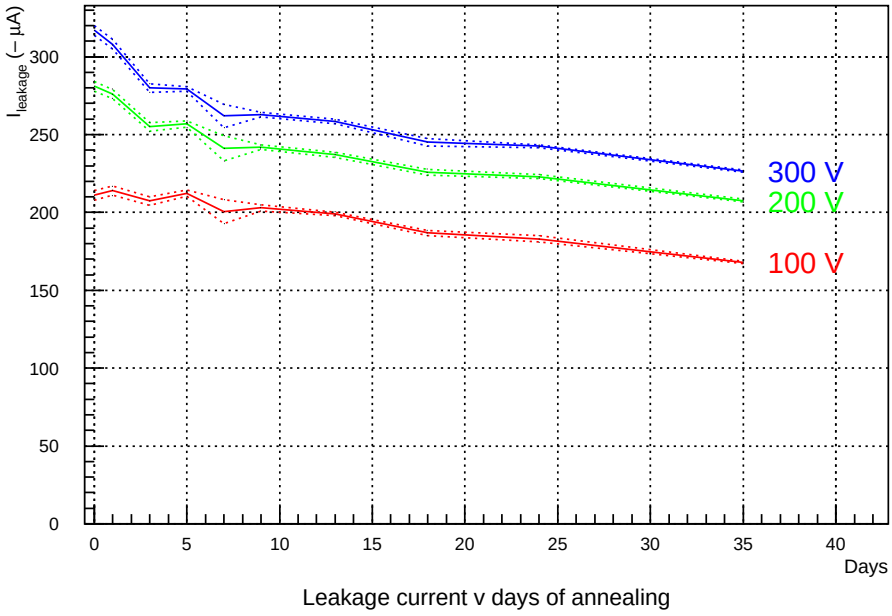

Figure 4: Leakage current of the detector at -10°C after irradiation with a dose of $2 \cdot 10^{14}$ protons/cm^2 as a function of the annealing time and for different reverse bias voltages. The current decreases with the elapsed annealing time. Solid lines indicate the mean value of the readings and the dashed lines the error bands.

2.5% in deconvolution mode. Also, the amount of charge collected in the cosmic ray run was found to be compatible with that obtained with a source run using the same detector. This charge has been estimated to be 3.6 fC, that is 22,500 electrons in a 300 μm thick detector.

For the same input signal, the response of the 6cm and 12cm-long channels differs. This is due to the larger capacitance of the 12cm channels, compared to that of the 6cm, Consequently the rise times of the signals coming out from the two detector regions are different. The disparate size of the output signal when using an identical input as calibrate leads to different calibration constants for the 6cm and 12cm regions. Therefore, to compare in a radioactive source run the real signals from each detector region, correction must be made according to the appropriate calibration constants.

The effect of the strip length on the output signal can be derived by changing the delay between the calibrate pulse injection and the system trigger. This method also allows the determination of the optimum delay giving the maximum response. Figures 5 and 6 show the different size of the calibrate output as a function of the delay time for the 6cm and 12cm channels, in peak and deconvolution mode respectively. The maximum output size is lower in the 12cm region for both operating modes. The effect is more pronounced in deconvolution mode.

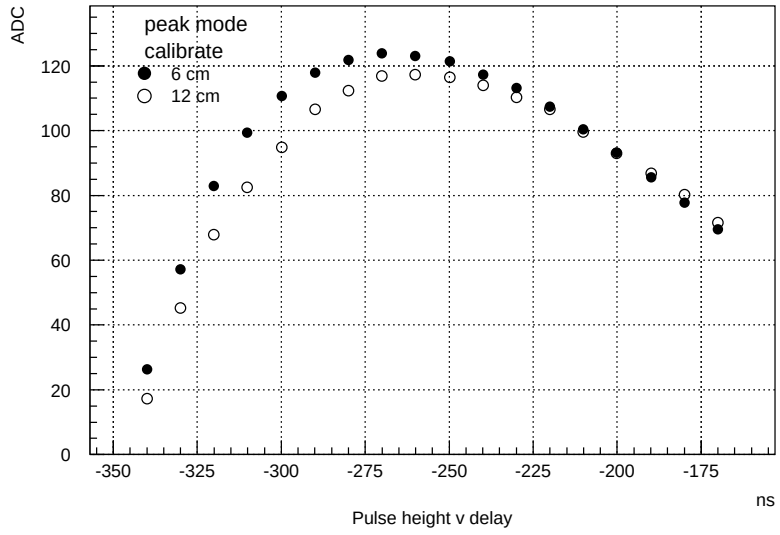

Figure 5: Calibration and timing in peak mode.

3.3 Noise

The single channel noise has been already presented in figure 2. As shown in that figure, all the channels which belong to the same group have similar noise. The dependence on the bias voltage of the mean noise per group in peak mode is shown in figure 7 and for an irradiated detector (no annealing accumulated). The figure shows that the noise does not exhibit a drastic reduction when the detector is fully depleted, as it would do it if the detector still had an n-type bulk [11]. This effect is consistent with the radiation damage having inverted the bulk type from n-type to p-type [3].

The noise figures obtained with the detector which has been used all along this study show no breakdown occurring below 600V (figure 7). This observation was further confirmed after 35 days of annealing. These results demonstrate that the irradiated n^+n silicon detectors can be safely operated at high bias voltages.

The noise is seen to increase with the bias voltage (i.e. leakage current), but this dependence is very small (see figure 7) and the noise can be considered constant for practical purposes.

The same analysis was repeated with a second detector irradiated with the same dose and stored under the same temperature conditions than the previous one, but not subjected to annealing. The results are presented in figure 8 where a sharp increase of the noise is observed for reverse bias voltages higher than 450 V. It is not clear if this burst on noise is related with a increase on the detector current (read section 3.1) indicating the production of micro-discharges or with the break down, as the leakage current (not shown) does not exhibit a change of the same magnitude than the noise [7],

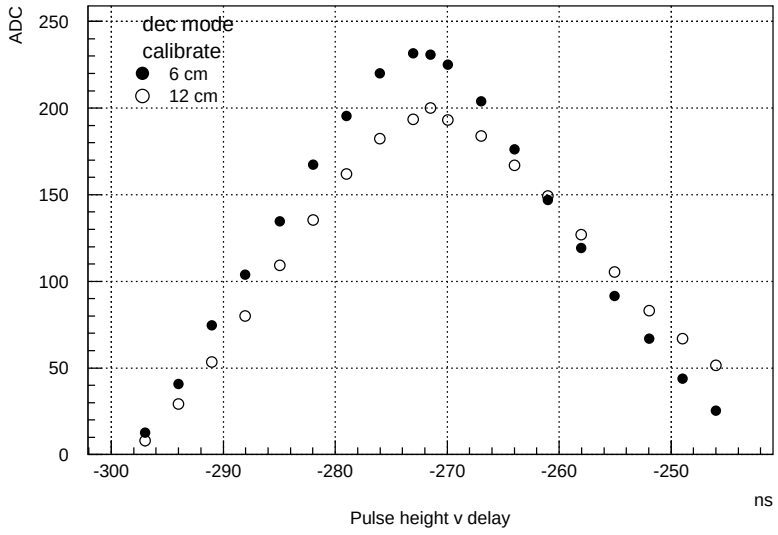

Figure 6: Calibration and timing in deconvolution mode.

but follows a similar behaviour of that shown in figure 3.

There was some concern in what way the angle between the polysilicon resistor and the implant may provoke micro-discharges. In the middle of the detector, the polysilicon resistor and implant run parallel each other, but close to the detector's edge they are at an angle due to the fan distribution of the strips. Those channels right to the edge were bonded to the electronics and the same study was repeated. The outcome was exactly the same, thus rejecting any suggestions that the angle between the polysilicon resistor and the implant influence the micro-discharge.

The noise does not depend on the annealing as consistent values were found through the whole annealing period. At 200 V and in peak mode it was estimated to be roughly 890 and 1250 electrons in the 6cm and 12cm region respectively (figure 2), while in deconvolution the noise was estimated to be 1310 and 1810 electrons respectively.

These figures of the noise level are required to extract the signal to noise ratio achievable by irradiated n^+n detectors. In the case where all 22,500 electrons are collected (i.e. no charge loss) and for a 12cm full size module, one can expect the maximum signal to noise in peak mode to be 18:1 and 13:1 in deconvolution. However the true figures for the real detectors also depend on the charge collection efficiency (section 3.4.2).

3.4 Charge Collection and Signal to Noise Ratio

This section is devoted to the study of the charge collection efficiency of the irradiated prototype. The detector was placed under a ^{106}Ru source, and then the signals produced by minimum ionizing particles crossing the detector were analyzed. Data was

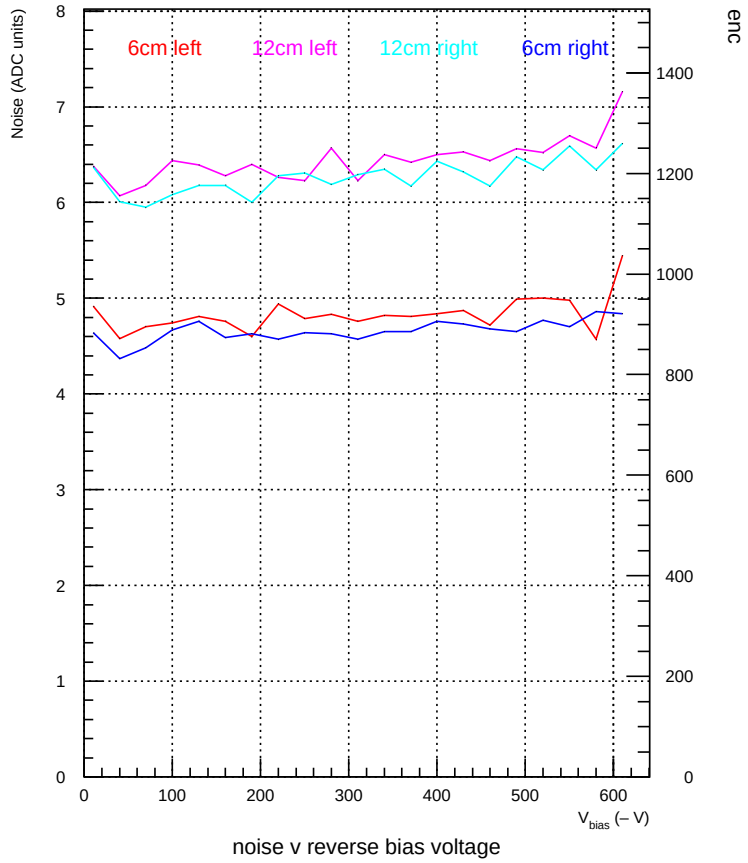

Figure 7: Noise in peak mode as a function of the detector bias voltage. Each curve corresponds to each of the four groups of channels.

collected in peak and deconvolution mode over a wide range of biasing voltages. The same measurements were repeated after every annealing cycle.

3.4.1 Cluster Search

In each event the impact point of the incident particle and its charge deposition are obtained from a cluster search through all 128 FELIX channels that proceeds as follows:

1. The strip significance (s_i = charge collected / noise, of the i-th channel) is computed for every single channel.
2. The *primary strip* is defined as the channel with the highest strip significance, provided that $s_{\rm ps} > 4$.
3. Up to five nearest neighbours of the primary strip are included in the cluster if

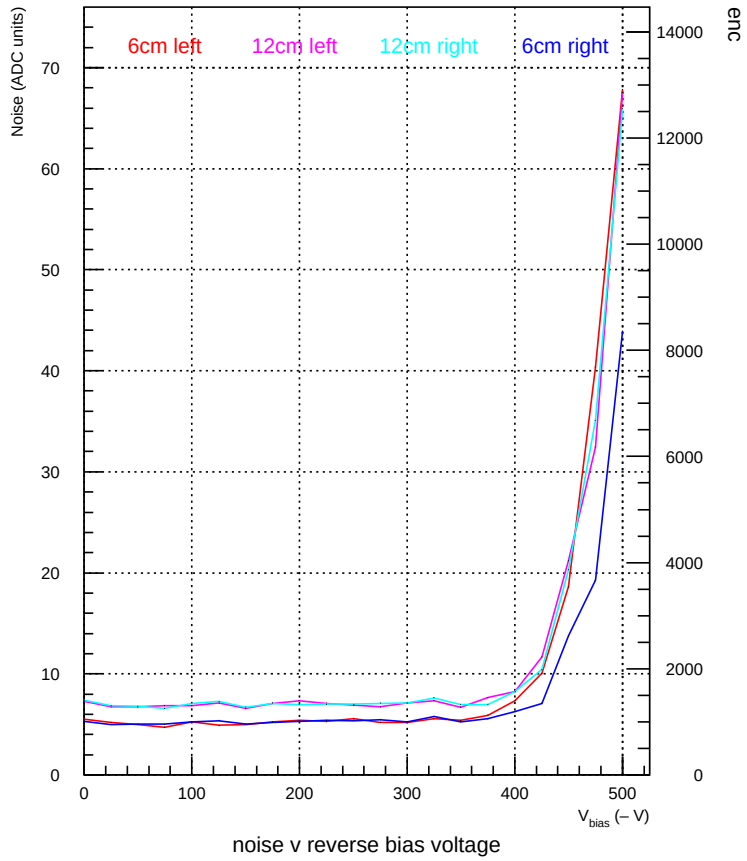

Figure 8: Noise in peak mode as a function of the detector bias voltage. Each curve corresponds to each of the four groups of channels. The noise has an onset for $V_{\rm bias}$ >450 V.

$s_{\rm neig} > 2$.

4. The *cluster significance* is defined as the sum of the significance of all strips included in the cluster. The cluster is required to have a significance ≥ 5.
5. Only those events with a single cluster are retained for the analysis.

The clusters selected with this procedure constitute the sample used in order to evaluate the charge collection efficiency, signal to noise ratio and full charge collection voltage.

Note that the cluster search method explained here was applied in exactly the same way for both types of collected data: peak and deconvolution.

3.4.2 Charge Collection Efficiency

The collected charge in each event is defined as the integral of the charge of all the strips in the cluster. Figure 9 shows the Landau distributions of the collected charge in the 6cm and 12cm regions. The peak of the charge distribution is fitted to a Gaussian, and it is considered as the peak of the Landau distribution. This procedure was found to be more robust than simply fitting a Landau, specially at low voltages where the signal drops down into the noise tail.

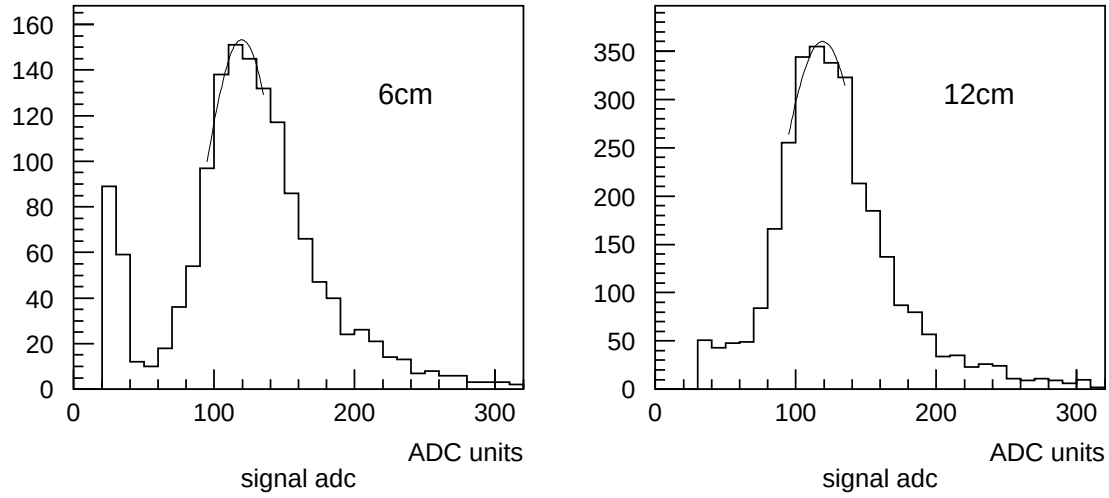

Figure 9: Landau distribution of the collected charge running in peak mode, with an irradiated detector subject to 18 days of annealing and biasing the detector with 250 V. The data collected with the 6cm-long (12cm-long) channels is presented in the left (right). Note the fit of the distribution's peak.

For unirradiated single sided n-type detectors, charge collection is only possible if the detector is fully depleted. On the other hand, charge collection in a p-type bulk detector is possible with a detector partially depleted, as charge collection is a linear function of the width of the depletion region, which varies as $V_{\rm bias}^{1/2}$. Accordingly, after the bulk type inversion due to the radiation damage [3], the collected charge of the n^+n detectors will grow as $V_{\rm bias}^{1/2}$ up to the voltage needed for full depletion [11].

Figures 10 and 11 present how the peak of the Landau distribution of the charge collection varies as a function of the reverse bias voltage in both peak and deconvolution mode respectively. Then the collected charge (q) is fitted to the following function:

$$q(V_{\rm bias}) = \begin{cases} a \cdot V_{\rm bias}^{1/2} & \text{if } V_{\rm bias} < V_{\rm fcc} \\ a \cdot V_{\rm fcc}^{1/2} & \text{otherwise} \end{cases} \qquad (1)$$

where $V_{\rm fcc}$ is the *full charge collection* voltage and a a conversion coefficient. In this way, the fit provides the value of $V_{\rm fcc}$, that is the minimum voltage at which the read out

electronics is believed to collect the maximum amount of charge and above which the charge collection efficiency remains constant [12]. The fit also gives direct information on the total charge collected once the detector is operated at or above $V_{\rm fcc}$.

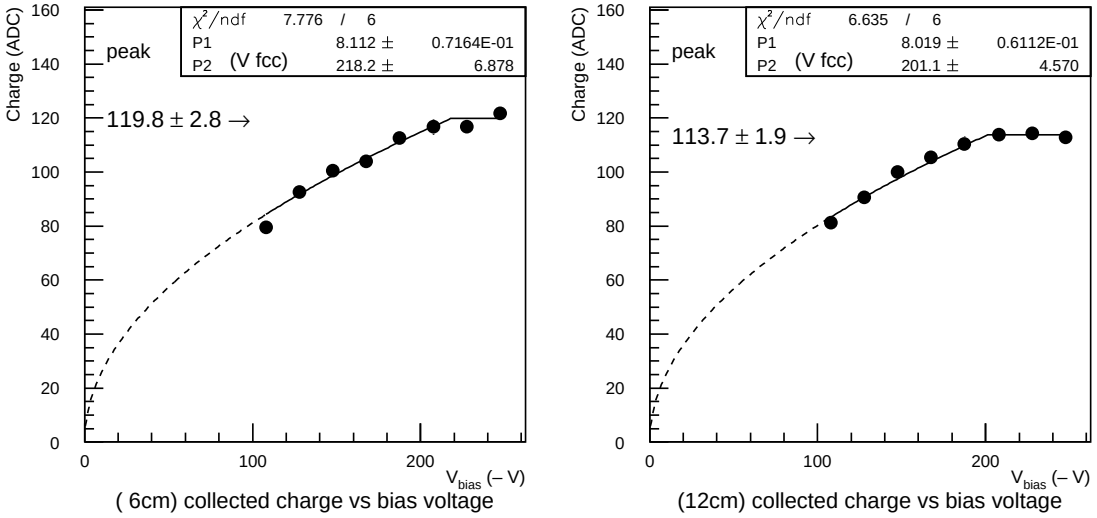

Figure 10: Charge collection (peak of the Landau distribution) as a function of the reverse bias voltage for data collected in peak mode with an irradiated detector with $2 \cdot 10^{14}$ protons/cm^2 and after 13 days of annealing at 20°C. On the right data collected in the 6cm region and left the 12cm. The fit results to equation 1 are also shown.

In both cases (peak and deconvolution mode) once the charge collection *plateau* is reached ($q_{\rm fcc}$), the value of $q_{\rm fcc}$ expressed in ADC counts is significantly higher in the 6cm region than in the 12cm region. This result was foreseen. The difference was explained in section 3.2 and underlines the importance of calibrating each region independently.

In the example given in figure 10, the total amount of charge collected in peak mode, once corrected with the appropriate calibration constant for each region, is found to be: $22,100 \pm 600$ electrons for the 6cm-long channels and $21,900 \pm 500$ e for 12cm. Both figures agree within errors.

The same behaviour is seen in deconvolution mode (figure 11). The total amount of electrons collected in the 6cm and 12 cm regions are: $18,800 \pm 600$ and $19,100 \pm 500$ respectively. Again both figures are in nice agreement.

Although there is accordance between the charge collected in the 6cm and 12cm regions, the figures do not reach the expected 22,500 e. It was considered the possibility of recovering the charge loss in deconvolution mode by using very high bias voltages. In this case the strong electric field will speed up the charge collection, thus restoring any ballistic deficit. However, running in deconvolution mode and biasing with 400 V, 500 V

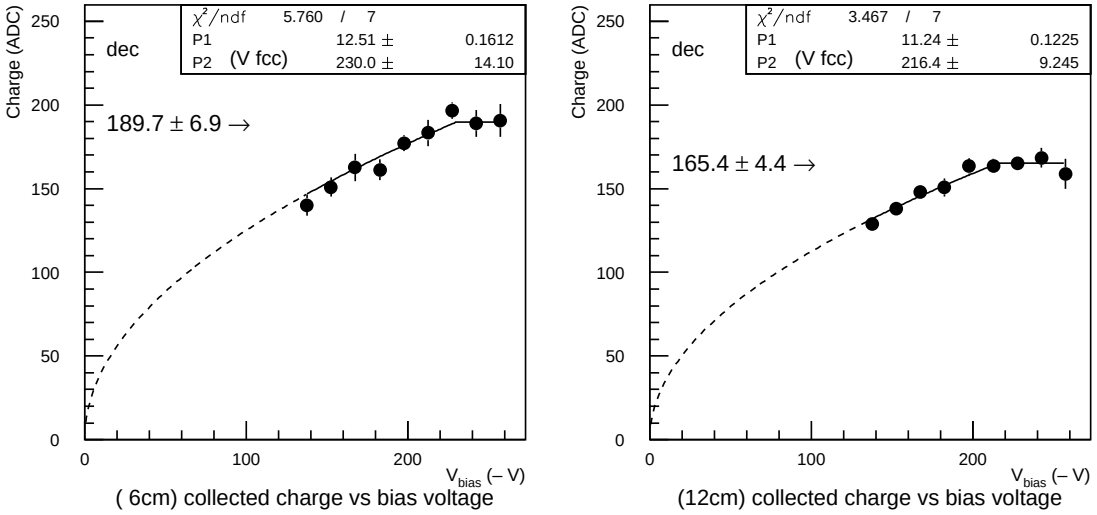

Figure 11: Charge collected (peak of the Landau distribution) as a function of the reverse bias voltage for data collected in deconvolution mode with the irradiated detector and after 13 days of annealing. On the right data collected in the 6cm region and left the 12cm. The fit results to equation 1 are also shown.

and 600 V, the charge collection efficiency did not shown any significant improvement. Therefore the charge loss inside the detector's volume is due to trapping. Trapping centres are one of the effects of the radiation damage in the bulk. Although the trapped carriers will be released later, the currents will be extended in time, thus affecting the response of the pre-amplifier and shaper, which leads to a ballistic deficit.

The charge collection efficiency is a critical factor when evaluating the global performance of the detector. Consequently, the possible effect of the annealing on the charge collection efficiency has been analyzed. The results of this investigation are presented in figure 12. There is no evidence of a dependence of the charge collection efficiency on the annealing time as it remains constant through all the annealing cycles. This is true for both FELIX read out modes. Figure 12 also compares the efficiency in both modes and it may be seen that it is higher in peak mode (98.8 $\pm$ 1.1 %) than in deconvolution mode (86.3$\pm$ 2.6 %). These figures represent a total number of 22,230 $\pm$ 250 and 19,420 $\pm$ 580 electrons.

As charge collection does not depend on the annealing time, it is very likely that the charge trapping centres are due to the permanent radiation damage.

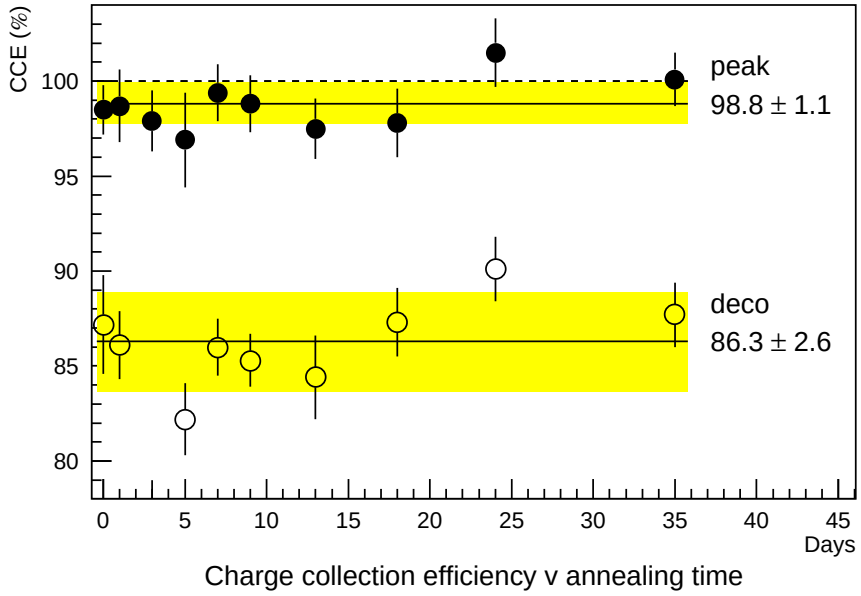

Figure 12: Charge collection efficiency *versus* the annealing time. The solid lines represent the mean value and the shadowed area the error band. A systematic error of 1% (2.5%) is included accounting for the uncertainty in the calibration pulse in peak (deconvolution) mode.

3.4.3 Signal to Noise Ratio

The *signal to noise ratio* is taken as the peak of the cluster significance distribution (figure 13). The values obtained in this work for the signal to noise ratio depend basically on the following factors:

- data sampling time (i.e. peak or deconvolution mode),
- bias voltage,

Previous studies using the FELIX chip [11, 13] have shown that, as expected, its performance in peak mode is better than using deconvolution mode (section 2). This fact is to a large extent due to the higher noise level recorded in deconvolution mode as consequence of the triple correlated sampling of consecutive 25 ns time slots needed to produce an effective deconvolution of the 75ns shaping time.

The influence of the reverse bias voltage is studied through its effect on the charge collection (as already mentioned in section 3.4.2 and shown in figures 10 and 11) and on the noise. Obviously, a bias voltage high enough in order to ensure an optimum charge collection is desired. Nevertheless other constraints may litigate against the use of high biasing voltages, for example to avoid problems of power consumption, high currents, excessive heating, micro-discharge (although this seems not to be an issue up

to $V_{\text{bias}} > 450$ V, section 3.3), bad regions or concerns of operate at high voltage due to risk of beam splash.

To derive the best performance of the irradiated detector, the results presented in this section are obtained by applying voltages above those needed for maximum charge collection.

Figure 13 shows the Landau distribution of the cluster significance for data collected in deconvolution mode. In that figure the 6cm region is giving a signal to noise ratio of 15:1, while the 12cm channels provide a signal to noise ratio close to 11:1.

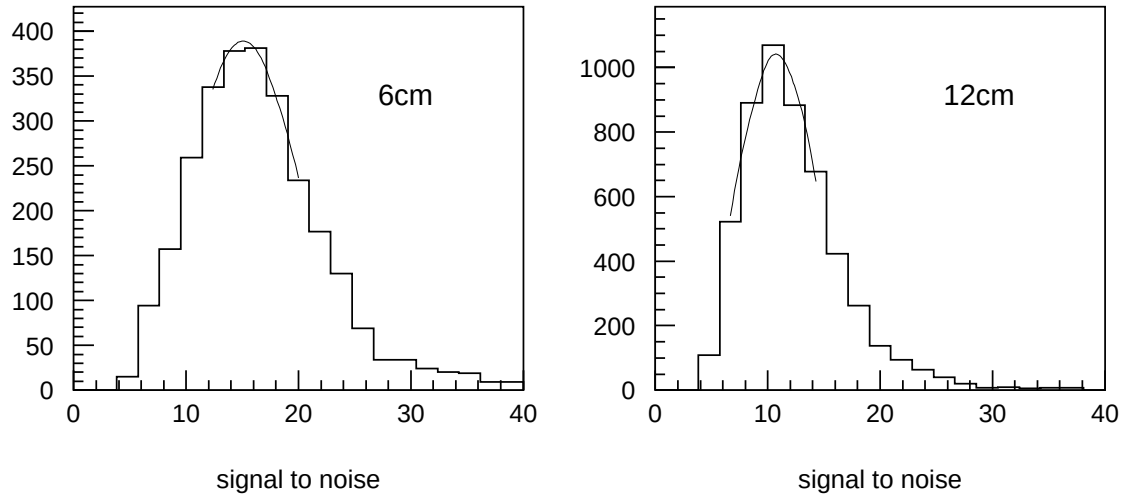

Figure 13: Landau distribution of the signal to noise ratio for data taken in deconvolution mode at 300 V with the irradiated detector and after 35 days of annealing.

In peak mode, according to the amount of charge collected and the noise of the 6cm and 12cm regions, the signal to noise ratios are found to be 25:1 and 18:1 respectively. The results in this mode are better, not just because the noise is lower but also because the charge collection efficiency is also higher.

The signal to noise figures above depletion presented through this section do not exhibit any dependence on the elapsed annealing time. This result was expected as that is the behaviour that follow both signal and noise. Therefore, the annealing neither improve nor degrade the performance of an irradiated detector in terms of the signal, noise and signal to noise.

3.5 Full Charge Collection Voltage

On irradiated detectors, the *full charge collection voltage* (i.e. the reverse bias voltage at which the maximum charge collection is reached) may differ from the depletion voltage as estimated from standard CV measurements.

Figure 14 represents the CV measurements on the detector after 3 days of annealing and performed at different frequencies. That plot shows that only low frequencies are suitable in order to determine the depletion voltage of the irradiated detectors. The depletion voltage found using 100 Hz is close to 200 V. It is experienced that the CV characteristics does not follow exactly the expected $V^{-1/2}$ behaviour to a large extent due to a growing of the series resistance of the undepleted bulk [5, 12].

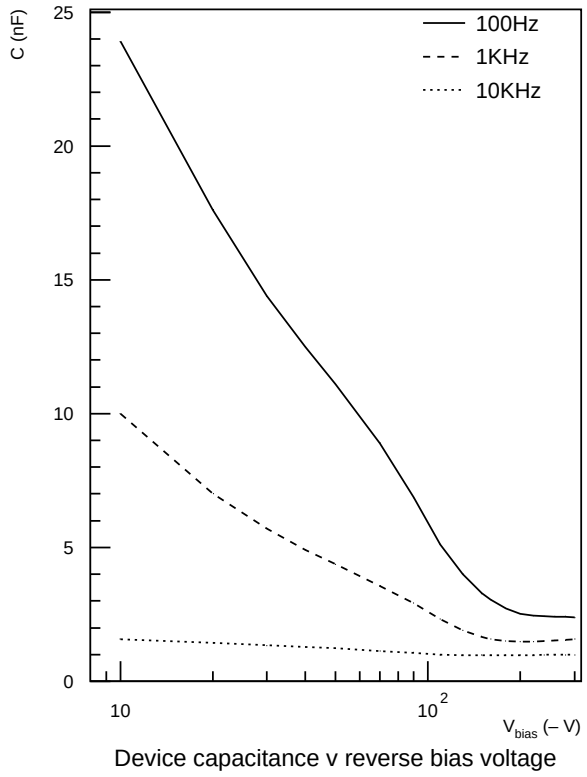

Figure 14: CV characteristic plot after 3 days of annealing. The depletion voltage is seen to be close to 150 V. However at this voltage not all the charge is collected.

The first consequence of the radiation damage is a net increase of the depletion voltage from 50 V (prior irradiation) up to 200 V. The variation of the depletion voltage of an irradiated detector is due to change of the effective doping concentration by generating acceptor-like states and removing donors. This explains why after large doses the bulk effective doping concentration may change from predominantly donors to acceptors, thus inverting the bulk type.

On the other hand, the full charge collection voltage as obtained by fitting the distributions of the signal as a function of the reverse bias voltages is seen to be 238 ± 5V, that means almost 30V above the depletion voltage given by the CV measurements.

The fit of the charge collection as a function of the bias voltage (e.g. figures 10 and 11) allows extracting a corresponding value for peak and deconvolution mode ($V_{\rm fcc}^{\rm peak}$ and $V_{\rm fcc}^{\rm deco}$) by combining their respective values for the 6 cm and 12 cm regions. The $V_{\rm fcc}^{\rm peak}$ and $V_{\rm fcc}^{\rm deco.}$ give similar values through all the annealing cycles. Therefore a common value for $V_{\rm fcc}$ is adopted as the weighted mean of $V_{\rm fcc}^{\rm peak}$ and $V_{\rm fcc}^{\rm deco}$.

The depletion voltage of an irradiated detector varies with the elapsed annealing time. For short annealing times, the depletion voltages decreases very quickly till it reaches a minimum. Then it starts growing again as the detector is subject to reverse annealing. That change is associated to the variation of the concentration of damage induced acceptor-like states.

The experimental results obtained for $V_{\rm fcc}$ as a function of the annealing time are presented in figure 15. The experimental points for the $V_{\rm fcc}$ are fitted to the following function:

$$V(t) = V_{\rm short}(t) + V_{\rm long}(t) + V_{\rm perm} \tag{2}$$

where the individual parametrization of the short ($V_{\rm short}$) and long term annealing ($V_{\rm long}$) is given by:

$$\begin{aligned} V_{\rm short}(t) = &\quad V_{s0}\exp(-t/\tau_s) \\ V_{\rm long}(t) = &\quad V_{l0}\left(1+\tfrac{1}{1+V_{l0}\cdot t/\tau_l}\right) \end{aligned}$$

while the permanent damage contribution ($V_{\rm perm}$) is taken as constant.

In this way, the short term annealing reduces the acceptor concentration exponentially with a τ_s lifetime (4 days approximately according to the parametrization and fit results). Then it passes through a minimum at 211 V after 11 days of annealing (in agreement with that reported in references [10, 14]). The long term reverse annealing will increase the value of $V_{\rm fcc}$, which will eventually saturate at 254 V (see table 3).

Table 3: Fit results of $V_{\rm fcc}$ to equation 2.

χ^2/ degrees of freedom	3.8/5	
$V_{\rm fcc}$ just after irradiation	272	V
Minimum value of $V_{\rm fcc}$	211	V
Reached after days of annealing	11	days
Saturation value of $V_{\rm fcc}$ (long term)	254	V
Permanent damage ($V_{\rm perm}$)	104	V

From the detector operation point of view, what matters is just the charge collection and not the depletion voltage *per se*. This is the reason why this study pays more attention to the full charge collection voltage than to the determination of the depletion voltage with standard CV measurements.

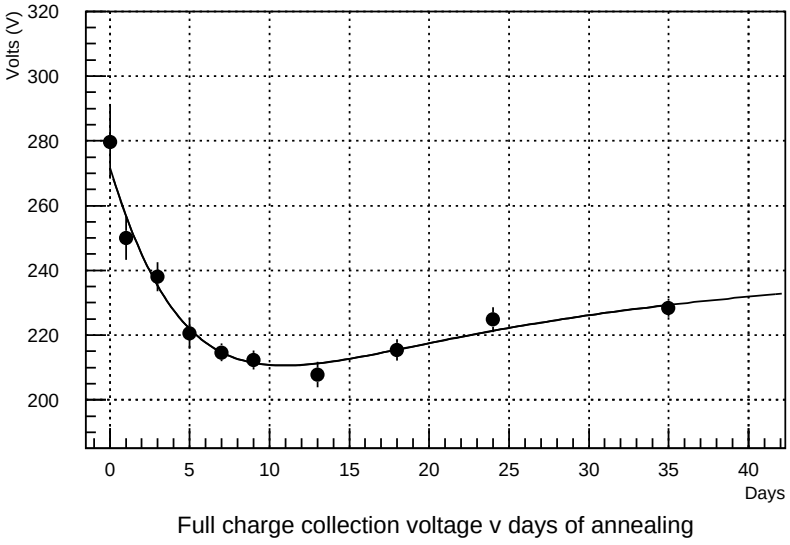

Figure 15: Full charge collection voltage as a function of the annealing time, fitted to equation 2.

3.6 Relative efficiency

Another point of interest is the particle detection efficiency of the irradiated detectors. Unfortunately, with our lab system it is not possible to obtain the absolute efficiency, but just the relative efficiency when comparing the total amount of particles detected varying the operating conditions. The interest resides in proving that the partially depleted detector can provide a sufficiently high particle detection efficiency to give adequate performance for tracking.

The data analysis here was different to that explained in section 3.4.1. In this particular study, a binary-like analysis was adopted. The reason for that is because it allows to set quite easily the same threshold (1 fC in what follows) in both FELIX read out modes which have different intrinsic noise (section 3.3). So, the cluster search was as follows:

- The primary strip was defined as that one with the highest amount of charge ($q_{\rm ps}$), provide that $q_{\rm ps} > 1$ fC.
- Up to five nearest neighbours of the primary strip were included in the cluster if $q_{\rm neig} > 1$ fC.
- Only those events with a single cluster were selected.

The *relative efficiency* at a given voltage was estimated taking data with the radioactive source. It was computed as the number of events in which a cluster was found, compared to the mean of events with a cluster found in all the runs taken with the detector over-depleted (i.e. applying voltages higher than $V_{\rm fcc}$).

The impact of the partial depletion on the efficiency is different for each mode (figure 16). In that figure the relative efficiency (as defined above) is plotted for data collected in peak and deconvolution mode, for different biasing potentials and for an irradiated detector which has accumulated 35 days of annealing. One can appreciate how the relative efficiency increases with $V_{\rm bias}$. It is lower in deconvolution mode, undoubtfully due to the lower charge collection as the threshold is kept the same in both modes (1 fC).

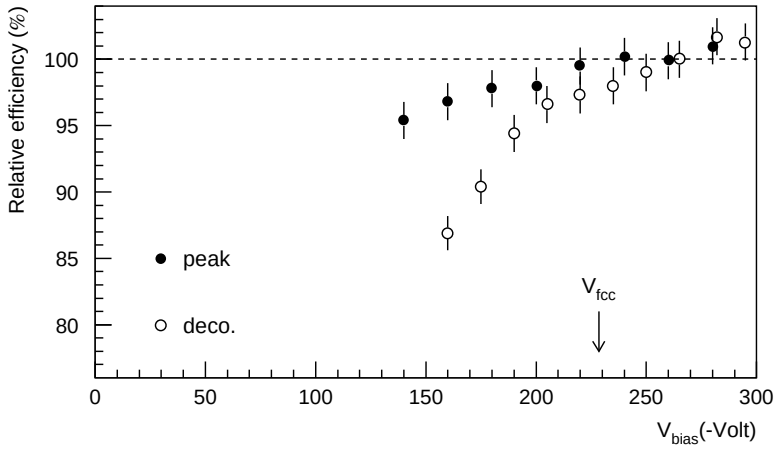

Figure 16: Relative efficiency of the irradiated detector and after 35 days of annealing.

Figure 16 shows that in deconvolution mode, the relative efficiency steadily increases even for $V_{\rm bias} > V_{\rm fcc}$. This is understood in terms of the charge division. High biasing voltages reduce the drift of the carriers. Consequently the same amount of charge is concentrated in fewer channels, thus increasing their probability of being asserted. This is confirmed by the amount of charge collected by the primary strip when using $V_{\rm bias} > V_{\rm fcc}$. For example, after 35 days of annealing $V_{\rm fcc}$ was 229 ± 3 V (figure 15) and of the 19,420 electrons collected in deconvolution mode, the primary strip it self collected $14,800 \pm 300$ at 235 V. Compare this with the $15,200 \pm 400$ e at 295 V and $16,500 \pm 700$ e at 600 V.

4 Summary and conclusions

The performance of the ATLAS n^+n silicon micro-strip detectors irradiated with $2 \cdot 10^{14}$ protons/cm^2 has been studied using the FELIX analogue read out chip. The tested prototype was subject to annealing for a period lasting 35 days at 20°C.

After the primary radiation damage, which induced an increase in the reverse current of two orders of magnitude, the annealing of the detector has reduced the total current by a 25% at 200V.

The short term annealing has a beneficial effect on the full charge collection voltage ($V_{\rm fcc}$). The minimum for $V_{\rm fcc}$ was found after 11 days of annealing. Afterwards, a slight increase of $V_{\rm fcc}$ is observed under the effect of the harmful long term annealing.

In addition, annealing does not alter the performance of the irradiated detectors as the size of the signal does not exhibit any dependence with the annealing time. The same is true for the noise in the detector. Therefore the signal to noise remains constant. Table 4 summarises the results for the signal, noise and signal to noise.

Table 4: Charge collection, the noise and the signal to noise of an irradiated n^+n silicon detector.

mode	signal(e)	noise(e)		signal to noise	
		6 cm	12 cm	6 cm	12 cm
peak	$22,230 \pm 250$	890 ± 20	1250 ± 24	25:1	18:1
deco.	$19,420 \pm 580$	1310 ± 40	1810 ± 62	15:1	11:1

It has been proved that the n^+n detectors can be safely operated at high voltages as no micro-discharge has been observed in this device, neither by burst on the leakage current, nor by a onset of the noise, and for operational voltages below the depletion voltage. Two devices has been operated successfully at very high voltages (above 400 V), although the noise at $V > 450$ V can indicate the production of breakdown in only one of the devices.

Due to radiation damage, the charge collection efficiency is reduced to a 99% in peak and a 86% in deconvolution mode. The charge loss is not recovered by applying very high voltages (up to 600V). The charge loss is seen to occur in trapping centres.

References

[1] ATLAS col. "ATLAS Technical Proposal". CERN/LHCC/94–43, 1994.

[2] D. Pitzl et al. "Type inversion in silicon detectors". *Nucl. Inst. and Meth. A*, 311:98–104, 1992.

[3] T. Schulz. *Investigation of the long term behaviour of the dammage effects and corresponding defects in detector grades silicon after neutron irradiation.* PhD thesis, Universität Hamburg, January 1996.

[4] J.A.J. Matthews et al. "Bulk radiation damage in silicon detector and implications for LHC experiments". *Nucl. Inst. and Meth. A*, 381:338–348, 1996.

[5] H. Feick. *Radiation tolerance of silicon particle detectors for High-Energy Physics experiments.* PhD thesis, Universität Hamburg, August 1997.

[6] S.J. Bates et al. "Recent results of radiation damage studies in silicon". *Nucl. Inst. and Meth. A*, 344:228–236, 1994.

[7] T. Ohsugi et al. "Micro-discharges of AC-coupled silicon strip sensors". *Nucl. Inst. and Meth. A*, 342:22–26, 1994.

[8] RD 20 Coll. "RD20 Status report presented to the DRDC". CERN/DRDC–94–39, 1994.

[9] S. Gadomski et al. "The deconvolution method of fast pulse shaping at hadron colliders". *Nucl. Inst. and Meth. A*, 340:217–227, 1992.

[10] F. Lemeilleur et al. "Study of characteristics of silicon detectors irradiated wit 24 GeV/c protons between -20°C and +20°C". *Nucl. Inst. and Meth. A*, 360:438–444, 1995.

[11] P.P. Allport et al. "Performance of the ATLAS-A silicon detector with analogue read out". ATLAS INDET–NO–133, hep–ex/9606012, 1996.

[12] M. Edwards et al. "Neutron radiation damage studies of silicon detectors". *Nucl. Inst. and Meth. A*, 310:283–286, 1991.

[13] P.P. Allport et al. "Studies of resolution, efficiency and noise for different front end trheshold algorithms using ATLAS-A silicon detector test beam data". ATLAS INDET–NO–131, 1996.

[14] Z. Li. "Investigation on the long-term radiation hardnees of low and medium resistivity starting silicon materials for RT silicon detectors in HEP". *Nucl. Inst. and Meth. A*, 360:445–454, 1995.